Electron Exchange Luminescence of Spiroadamantane-Substituted Dioxetanes Triggered by Alkaline Phosphatase. Kinetics and Elucidation of pH Effects

Waldemar Adam,[†] Irena Bronstein,[‡] Brooks Edwards,[‡] Thomas Engel,[§] Dirk Reinhardt,[†] Friedemann W. Schneider,[§] Alexei V. Trofimov,*[,†,||] and Rostislav F. Vasil'ev[||]

Contribution from the Institute of Organic Chemistry, University of Würzburg, Am Hubland, D-97074 Würzburg, Germany, Tropix, Inc., 47 Wiggins Avenue, Bedford, Massachusetts 01730, Institute of Physical Chemistry, University of Würzburg, Marcusstrasse 11, D-97070 Würzburg, Germany, and Institute of Biochemical Physics, United Institute of Chemical Physics, Russian Academy of Sciences, ul. Kosygina 4, Moscow 117977, Russia

Received June 6, 1996[⊗]

Abstract: Intramolecular chemically initiated electron exchange luminescence (CIEEL) was studied in the alkaline phosphatase triggering of the spiroadamantyl-substituted 1,2-dioxetanes **AMPPD** and **CSPD**, which are widely employed in modern chemiluminescent bioassays, particularly in clinical immunoassay applications. Experimental data on the pH dependence of the CIEEL efficiency, the CIEEL emitter fluorescence lifetime, the rate of cleavage of the dephosphorylated dioxetane **2a**, the turnover number, and the Michaelis constant are reported and kinetically rationalized. Through this detailed kinetic analysis, the pH effects on the various steps of the CIEEL process were elucidated. Although every step of the triggering involves H^+ or HO^- ions, it was shown that at alkaline pH and steady-state conditions only enzymatic dephosphorylation of **AMPPD** and **CSPD** depends on pH in this CIEEL process. The turnover number is affected only at pH below 9, which reflects a switchover of the rate-determining step of the enzyme dephosphorylation to its phosphorylation at increasing pH. The Michaelis constant depends on pH within the entire range used, which is attributed to the pH effect on the concentration of the catalytically active enzyme form. The present model kinetic studies on the important alkaline-phosphatase-triggered CIEEL reaction provide the necessary mechanistic insights to understand pH effects in such enzymatic processes for the rational design of more effective CIEEL systems.

Introduction

The chemiluminescence properties of dioxetanes as high-energy peroxides are of particular interest for the generation of excited states without light. The formation of electronically excited products can be induced either thermally or by an electron-transfer mechanism, originally discovered by Schuster for the diphenoyl peroxide[1] and in the meantime abundantly documented for the α-peroxy lactones[2] and appropriate dioxetanes.[3] This phenomenon of light emission derived from electron transfer chemistry is known as **c**hemically **i**nitiated **e**lectron **e**xchange **l**uminescence (CIEEL). At the reaction rate v, intensity of the CIEEL i^{CIEEL} may be expressed by eq 1, in which $\Phi^{CIEEL} = \Phi^*\Phi^{fl}$ is the CIEEL yield

$$i^{CIEEL} = \Phi^{CIEEL} v \qquad (1)$$

represented by the product of the chemiexcitation yield Φ^* (*i.e.*, yield of the excited reaction product, the CIEEL emitter) and the fluorescence efficiency Φ^{fl} of the CIEEL emitter.

The CIEEL may result from both intermolecular and intramolecular electron transfer. The latter case has been attributed, in particular, to the firefly luciferase-luciferin bioluminescence.[4] For this intramolecular CIEEL process the chemiluminescence quantum yield is over 90% *in vivo*, *i.e.*, chemical energy is efficiently converted into electronic excitation manifested by light emission.

Also 1,2-dioxetanes with substituents of low oxidation potentials such as the aryl-O^- functionality display intramolecular CIEEL. The chemiexcitation step consists of the cleavage of the intermediate dioxetane phenolate anion. Such cleavage is initiated by the intramolecular electron transfer from the oxidizable phenoxide functionality to the antibonding σ^* orbital of the peroxide bond. These phenolate-initiated intramolecular CIEEL processes provide the basis for numerous commercial applications, most prominently in chemiluminescent immunoassays. Numerous research efforts were undertaken to develop more efficient CIEEL systems for the above purposes. The most successful design[5,6] utilizes thermally persistent

* For convenience, correspondence should be send to Prof. Dr. Waldemar Adam, Institute of Organic Chemistry, University of Würzburg, Am Hubland, D-97074 Würzburg, Germany. Tel. +49 931 8885340/339. Telefax: +49 931 8884756. E-mail: adam@chemie.uni-wuerzburg.de.

[†] Institute of Organic Chemistry, University of Würzburg.

[‡] Tropix, Inc.

[§] Institute of Physical Chemistry, University of Würzburg.

[||] Russian Academy of Sciences.

[⊗] Abstract published in *Advance ACS Abstracts,* October 15, 1996.

(1) Koo, J.-Y.; Schuster, G. B. *J. Am. Chem. Soc.* **1977**, *99*, 6107−6109.

(2) Adam, W.; Cueto, O. *J. Am. Chem. Soc.* **1979**, *101*, 6511−6515.

(3) Adam, W.; Zinner, K.; Krebs, A.; Schmalstieg, H. *Tetrahedron Lett.* **1981**, *22*, 4567−4570.

(4) Koo, J.-Y.; Schmidt, S. P.; Schuster, G. B. *Proc. Natl. Acad. Sci. U.S.A.* **1978**, *75*, 30−33.

(5) (a) Bronstein, I.; Edwards, B.; Voyta, J. C. *J. Biolumin. Chemilumin.* **1988**, *2*, 186. (b) Edwards J. C.; Sparks, A.; Voyta, J. C.; Bronstein, I. *J. Biolumin. Chemilumin.* **1990**, *5*, 1−4. (c) Bronstein, I.; Edwards, B.; Voyta, J. C. *J. Biolumin. Chemilumin.* **1989**, *4*, 99−111.

(6) (a) Schaap, A. P.; Chen, T.-S.; Handley, R. S.; DeSilva, R.; Giri, B. P. *Tetrahedron Lett.* **1987**, *28*, 1155−1158. (b) Schaap, A. P.; Handley, R. S.; Giri, B. P. *Tetrahedron Lett.* **1987**, *28*, 935−938.

S0002-7863(96)01904-X CCC: $12.00

Scheme 1

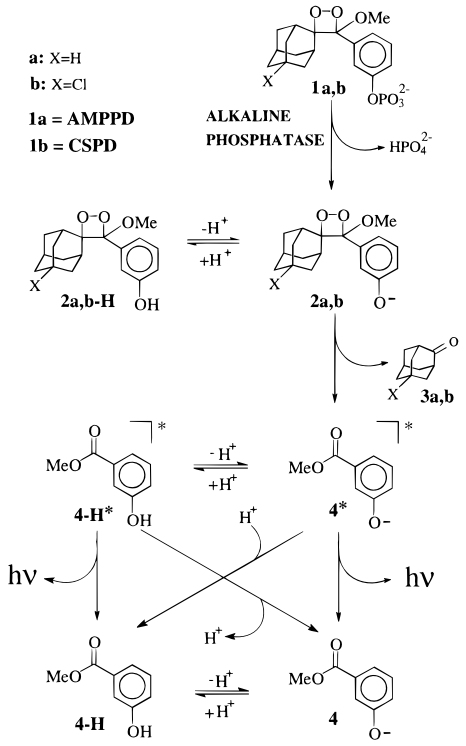

spiroadamantyl-substituted dioxetanes with a protected phenolate ion. The advantage of such spiroadamantyl-substituted dioxetanes is their thermal persistence and their convenient synthesis through photooxidation.[7] Our detailed kinetic study of the excited state formation in the thermal decomposition of such dioxetanes has been reported recently.[8]

The CIEEL of these dioxetanes can be generated at will on treatment with an appropriate reagent (trigger) to release the phenolate ion, which depends on the nature of the protective group. In early studies of the chemical[6] and enzymatic[5,6b] triggering, the phenolate moiety (*m*-oxybenzoate anion) was found to be the only excited-state decomposition product, hence the observed CIEEL represents fluorescence of the latter, which was confirmed by the CIEEL spectra.[5c,6]

Although the CIEEL phenomenon was intensively studied, most research efforts were undertaken to elucidate emissive species and plausible chemiexcitation pathways as well as to develop efficient CIEEL systems. A comprehensive kinetic theory of such important and fundamental phenomenon is still lacking. However, the mechanism and kinetics of the CIEEL generation need to be studied in detail, if further effective CIEEL-triggerable systems are to be rationally designed rather than empirically through trial and error. That is why we have undertaken model kinetic studies of the phenolate-initiated intramolecular CIEEL processes. Recently we have reported a kinetic study of the CIEEL in the decomposition of the silyloxy-substituted spiroadamantyl dioxetanes triggered by fluoride ions through the removal of the $SiMe_2tBu$ protective group.[9] In the present work we present the kinetic study of the enzymatic CIEEL process shown in Scheme 1. Through this work we intend to contribute to the development of the kinetic theory of the CIEEL phenomenon.

Kinetic Background and Analysis

In the case of the CIEEL process shown in Scheme 1, the phenolate functionality of the dioxetanes **1a** (**AMPPD**) and **1b** (**CSPD**) is protected by a phosphate group. The CIEEL cleavage of such dioxetanes may be triggered by alkaline phosphatase, in which the enzyme removes the phosphate group. This case constitutes the basic concept in the design of effective commercial chemiluminescence probes for clinical applications.[5,10,11] The alkaline phosphatase in most applications is attached to target biomolecules (proteins and nucleic acids) as a label or is expressed by a specific gene in reporter gene assays[11] and its catalytic action results in the dephosphorylation of the aryl phosphate moiety of the dioxetane to release the phenolate functionality (step **1** → **2**, Scheme 1), which subsequently triggers light emission by cleavage of the dioxetane ring to produce the electronically excited fluorophor (step **2** → **4***, Scheme 1).

Since every enzymatic CIEEL process is pH-controlled, it is very important to elucidate the pH dependence of the reaction kinetics. In Scheme 1, the variation of pH may affect (i) the CIEEL yield through changes of the fluorescence properties of the CIEEL emitter, (ii) the rate of cleavage of the intermediary dioxetane phenolate **2,** and (iii) the enzymatic dephosphorylation of the dioxetane **1**. The aim of the present study was to assess the pH effects on these different steps of this important CIEEL process.

Protonation of excited phenolate **4*** may result not only in the formation of the ground state phenol **4-H** but also in excited phenol **4-H*** species (Scheme 1) through adiabatic proton transfer.[12] Thus, apart from the influence on the **4*** fluorescence efficiency, variation of pH may result in a new CIEEL emitter, namely **4-H***. To verify the possible intervention of such a new emissive species, merely the pH dependence of the emission wavelengths needs to be checked.

As to the pH dependence of the fluorescence efficiency for the phenolate **4***, its measurement presents problems. In buffer solutions, the ground-state phenolate **4** is in equilibrium with the phenol **4-H** and since the absorption spectra of these two species are quite overlapped and the relative concentration of the **4** and **4-H** species is also dependent on pH, conventional measurements of the pH dependence of the steady-state fluorescence emission are unreliable because the amount of the emitter derived from **4** varies with pH in the equilibrium **4** ⇌ **4-H** (Scheme 1). To circumvent this problem, one needs to conduct time-resolved fluorescence measurements as function of pH. Since the fluorescence efficiency Φ^{fl} is given by $\Phi^{fl} = k^{fl}\tau$, *i.e.*, the product of the fluorescence rate constant k^{fl} and the fluorescence lifetime τ, pH changes of the fluorescence efficiency should be accessible through their effect on the fluorescence lifetime. Thus, in the present work the measurements of the phenolate **4*** fluorescence lifetime *versus* pH were to be performed.

Data on the CIEEL yield at various pH may be available through the measurements of the total amount of light emitted in the complete dioxetane decomposition at high alkaline phosphatase concentration. The total number of photons $N_{photons}$ emitted in the complete dioxetane decomposition is represented by the area under the CIEEL intensity curve. Since the time profile of the CIEEL intensity $i^{CIEEL}(t)$ is described by eq 1 and the area under such a curve is given by integration of $i^{CIEEL}(t)$

(7) Adam, W.; Arias, L. A.; Zinner, K. *Chem. Ber.* **1983**, *116*, 839−846.
(8) Trofimov, A. V.; Vasil'ev, R. F.; Adam, W.; Mielke, K. *Photochem. Photobiol.* **1995**, *62*, 35−43.
(9) Trofimov, A. V.; Mielke, K.; Vasil'ev, R. F.; Adam, W. *Photochem. Photobiol.* **1996**, *63*, 463−467.
(10) Beck, S.; Köster, H. *Anal. Chem.* **1990**, *62*, 2258−2270.
(11) Bronstein, I.; Fortin, J. J.; Voyta, J. C.; Juo, R.-R.; Edwards, B.; Olesen, C. E. M.; Lijam, N.; Krichka, L. J. *BioTechniques* **1996**, *17*, 172−177.
(12) Ireland, J. F.; Wyatt, P. A. H. *Adv. Phys. Org. Chem.* **1976**, *12*, 131−221.

Scheme 2

$$\mathbf{E}H_2^{2+} \underset{+H^+}{\overset{-H^+}{\rightleftharpoons}} \mathbf{E}H^+ \underset{+H^+}{\overset{-H^+}{\rightleftharpoons}} \mathbf{E}$$

over the reaction time, the expression for $N_{photons}$ is given by eq 2, in which

$$\int_0^\infty v\,dt$$

represents the total dioxetane concentration [**1**] decomposed by the enzyme. Therefore, from eq 2 it follows that the CIEEL yield Φ^{CIEEL} is determined by eq 3.

$$N_{photons} = \int_0^\infty i_{cat}^{CIEEL}\,dt = \Phi^{CIEEL}\int_0^\infty v_{cat}\,dt = \Phi^{CIEEL}[\mathbf{1}] \quad (2)$$

$$\Phi^{CIEEL} = \frac{N_{photons}}{[\mathbf{1}]} \quad (3)$$

The pH dependence of the enzymatic dephosphorylation of the dioxetanes **1** (step **1** → **2**, Scheme 1) derives from the pH influence on the rate-determining step of catalysis and the concentration of the catalytically active enzyme form.[13] The pH effect on the latter may consist of direct changes on the active center of the enzyme (Ser-O$^-$)[14] and indirect ones on the functionalities in the vicinity of the active center. In view of a complex nature of the pH influence on the active enzyme form, we simplify our qualitative approach by merely assuming that the catalytically active form $\mathbf{E}H^+$ of the enzyme undergoes inactivation both through protonation at decreasing and deprotonation at the increasing pH. Thus, the catalytically active form $\mathbf{E}H^+$ of the enzyme is in equilibrium with its inactive protonated ($\mathbf{E}H_2^{2+}$) and deprotonated (**E**) forms, as shown in Scheme 2. The same approach was recently applied to the description of the pH effect on horseradish peroxidase.[15]

To understand the pH influence on the catalysis by alkaline phosphatase at the molecular level, the mechanism of enzyme action needs to be examined in detail in terms of Michaelis−Menten kinetics. Although phosphatases from various sources at the same conditions reveal different catalytic parameters, the general features of the catalytic mechanism are similar.[14] After the formation of a noncovalent Michaelis complex between the enzyme and substrate molecule, the catalysis by alkaline phosphatase proceeds through the phosphoenzyme intermediate (phosphorylation of the enzyme).[16] Release of the free enzyme molecule from the phosphoenzyme occurs effectively at high pH, whereas at low pH this process is slow and thereby rate-determining.[17] The pH increase may cause a switchover of the rate-determining step from dephosphorylation of the enzyme to its phosphorylation[13] by the participation of HO$^-$ ions. Consequently, the simplest catalytic mechanism may be represented by Scheme 3, in which $\mathbf{E}H^+$ is the active enzyme molecule, $\mathbf{E}H^+\cdot\mathbf{1}$ is the Michaelis complex, and $\mathbf{E}H^+\cdot PO_3^-$ represents the phosphorylated enzyme. Furthermore, the substrate rephosphorylation step k_{-2} is also involved in Scheme 3, since this reaction is known and even used for the enzymatic

Scheme 3

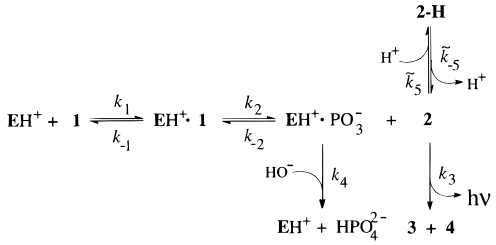

synthesis of phosphoric monoesters with alkaline phosphatase.[18] In addition to the cleavage k_3 and rephosphorylation k_{-2}, in aqueous buffer the deprotected dioxetane phenolate **2** undergoes reversible protonation (Schemes 1 and 3). In more detailed catalytic analyses, a distinction is made[14,17] between covalent binding and noncovalent association of the phosphate and the enzyme molecule; moreover, the isomerization of the Michaelis complex $\mathbf{E}H^+\cdot\mathbf{1}$ is considered.[19] However, such mechanistic details make the kinetic analysis of the enzymatic CIEEL process extremely complex. To simplify the kinetic analysis, we assume the simplified catalytic mechanism in Scheme 3 to rationalize the experimental results.

The pH effects on the rate-determining step of the catalysis and on the concentration of the catalytically active enzyme forms were expected to be reflected in both the catalytic rate constant (turnover number) k_{cat} and the Michaelis constant K_M. For this reason, these catalytic parameters were to be measured as function of pH.

For the determination of the catalytic parameters, steady-state conditions were to be employed in the kinetic analysis. Thus, when the enzyme concentration e_0 is much lower than [**1**], the rate-determining step of the overall CIEEL process is represented by the enzymatic dephosphorylation of the dioxetanes **1**. In this case, the reaction rate v_{cat} is expressed by the Michaelis−Menten rate law (eq 4). On substitution of eq 4 into eq 1, one obtains eq 6 for the CIEEL intensity at the steady-state conditions as a function of the dioxetane concentration. The linear form of eq 5 shown in eq 6 allows to obtain the catalytic parameters k_{cat} and K_M from the experimental dependence of the CIEEL intensity on the dioxetane substrate concentration [**1**]. The turnover number k_{cat} may be obtained from the intercept $(\Phi^{CIEEL}e_0\,k_{cat})^{-1}$ of the double-reciprocal plot of this dependence according to eq 6, since e_0 is known and Φ^{CIEEL} may be measured according to eq 3. Division of the slope of such a plot by its intercept gives the Michaelis constant K_M. These measurements performed at various pH allow one to obtain pH dependence of the catalytic parameters k_{cat} and K_M. To rationalize k_{cat} and K_M *versus* the pH experimental data in terms of Scheme 3, explicit forms of the pH dependence of these parameters need to be derived.

$$v_{cat} = \frac{k_{cat}e_0[\mathbf{1}]}{[\mathbf{1}] + K_M} \quad (4)$$

$$i_{cat}^{CIEEL} = \Phi^{CIEEL}c_{cat} = \frac{\Phi^{CIEEL}k_{cat}e_0[\mathbf{1}]}{[\mathbf{1}] + K_M} \quad (5)$$

$$(i_{cat}^{CIEEL})^{-1} = \frac{1}{\Phi^{CIEEL}k_{cat}e_0}\left\{1 + \frac{K_M}{[\mathbf{1}]}\right\} \quad (6)$$

(13) Jenks, W. P. *Catalysis in Chemistry and Enzymology*; McGraw-Hill, Inc.: New York, 1969; pp 487−490.
(14) Coleman, J. E.; Besman, M. J. A. In *Hydrolytic Enzymes*; Neuberger, A., Brocklehurst, K., Eds.; Elsevier Science Publishers B. V.: Amsterdam-New York-Oxford, 1987; pp 337−406.
(15) Holzbaur, I. E.; English, A. M.; Ismail, A. A. *J. Am. Chem. Soc.* **1996**, *118*, 3354−3359.
(16) Engström, L. *Biochem. Biophys. Acta* **1961**, *52*, 49−59.
(17) Chappelet-Tordo, D.; Fosset, M.; Iwatsubo, M.; Gache, C.; Lazdunski, M. *Biochemistry* **1974**, *13*, 1788−1795.
(18) Pradines, A.; Klaebe, A.; Perie, J.; Paul, F.; Monsan, P. *Tetrahedron* **1988**, *44*, 6373−6386.
(19) Gutfreund, H. *Enzymes: Physical Principles*; Wiley-Interscience: London-New York, 1972; pp 194−202.

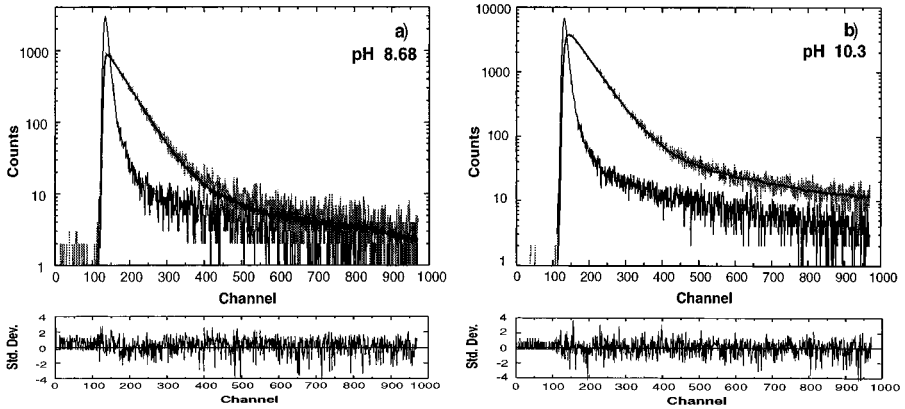

Figure 1. Fluorescence decay curves (λ_{ex} = 337 nm) and weighted residual plots of phenolate **4** ([**4**] + [**4-H**] = 10^{-4} M) in 0.05 M carbonate buffer, 1 mM $MgCl_2$, in the presence of 10^{-8} M alkaline phosphatase at (a) pH 8.68 (τ = 9.6 ns) and (b) pH 10.3 (τ = 10.3 ns) at room temperature (*ca.* 20 °C).

To permit an experimental distinction between the pH effects on the catalytic generation and the cleavage of the CIEEL-active dioxetane **2**, the kinetics of the base-induced CIEEL triggering of its protonated form **2-H** *versus* pH needed to be studied independently. The desired rate constant k_3 of the dioxetane **2** decomposition (Scheme 3) was to be obtained from the pseudo-first-order kinetics of the dioxetane **2-H** decay at high pH. Indeed, high pH causes rapid deprotonation of **2-H**, followed by the first-order CIEEL decay of **2**. The kinetics is described by eq 7, in which i_2^{CIEEL} represents the CIEEL intensity of **2**, and in logarithmic form it is expressed by eq 8. The rate constant k_3 is given by the slope of the plot of $\ln(i_2^{CIEEL})$ *versus* reaction time according to eq 8.

$$i_2^{CIEEL} = \Phi^{CIEEL} k_3[\mathbf{2}] = \Phi^{CIEEL} k_3[\mathbf{2\text{-}H}]_0 e^{-k_3 t} \qquad (7)$$

$$\ln(i_2^{CIEEL}) = \ln(\Phi^{CIEEL} k_3[\mathbf{2\text{-}H}]_0) - k_3 t \qquad (8)$$

Results

Fluorescence Lifetime of the CIEEL Emitter *versus* pH. The fluorescence decay curves at the lowest and highest pH used are shown in Figure 1. The decay curves at every pH were well fitted by monoexponential kinetics, which implies only one emissive species. This was also confirmed by the coincidence of the normalized emission spectra at the same pH values. The least-squares iterative deconvolution procedure applied to all of the decay curves afforded the fluorescence lifetimes of the phenolate **4** as a function of pH (Figure 2). All lifetime data in Figure 2 are the average of five measurements with low values of χ^2 (<1.1). Thus, at alkaline pH the fluorescence lifetime (*ca.* 10 ns) of the phenolate **4** is independent of pH (Figure 2).

CIEEL Yields *versus* pH. According to eq 3, the CIEEL yields were obtained through measurements of the total amount of light (areas under the CIEEL curves calibrated against the Hastings-Weber scintillation "cocktail" [20]) emitted in the complete decomposition of the **AMPPD** and **CSPD** at high alkaline phosphatase concentration (10^{-8} M). CIEEL curves at various pH are shown in Figure 3. Although at various pH the CIEEL reveals different kinetics (Figure 3), the areas under the CIEEL curves and, therefore, the CIEEL yields were found to be independent of pH within the experimental error (Figure 4). The values of the CIEEL yields are (7.5 ± 0.3) × 10^{-6} for the **AMPPD** and (5.7 ± 0.3) × 10^{-6} for the **CSPD**.

(20) Hastings, J. W.; Weber, G. *J. Opt. Am. Soc.* **1963**, *53*, 1410−1415.

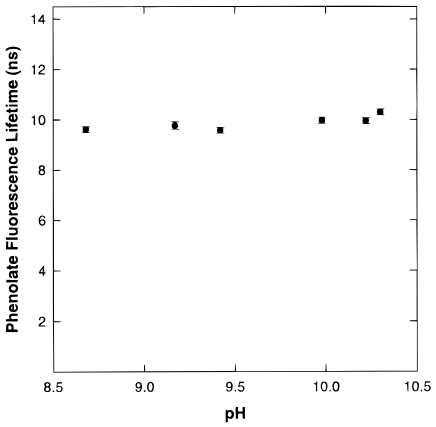

Figure 2. Fluorescence lifetime of the phenolate **4** ([**4**] + [**4**] = 10^{-4} M) *versus* pH in 0.05 M carbonate buffer, 1 mM $MgCl_2$ and in the presence of 10^{-8} M alkaline phosphatase at room temperature (*ca.* 20 °C).

Cleavage Kinetics of the Dioxetane Phenolate Anion. At pH > 12.6, the CIEEL decay was independent of pH in the base-induced triggering of dioxetane **2a-H**, and its kinetics followed the pseudo-first-order rate law for the cleavage of the dioxetane anion **2a** (Figure 5). From the linear plot of Figure 5, the rate constant k_3 of the dioxetane **2a** cleavage was found to be (1.2 ± 0.04) × 10^{-2} s^{-1} at 37 °C according to eq 8.

pH Dependence of the Michaelis Constant. The experimental dependences of the stationary CIEEL intensity on the **AMPPD** and **CSPD** concentrations measured at various pH are shown in Figures 6a and 7a. From the double-reciprocal plots according to eq 6 (Figures 6b and 7b), the value of the Michaelis constant was obtained for every pH value used. The experimental pH dependence of the K_M is shown in Figure 8, every point of which represents the average K_M value of four independent measurements for every particular pH.

Catalytic Rate Constant (Turnover Number). At pH 9.0−10.5 the intercepts of the double-reciprocal plots according to eq 6 (Figures 6b and 7b) and, consequently, the values of $\Phi^{CIEEL} e_0 k_{cat}$ are independent of pH for both **AMPPD** and **CSPD**. The latter values were found to be (1.9 ± 0.3) × 10^{-14} Ms^{-1} for **AMPPD** and (1.22 ± 0.21) × 10^{-14} Ms^{-1} for **CSPD** at 4.7 × 10^{-13} M alkaline phosphatase and 37 °C. On substitution of the measured CIEEL yields Φ^{CIEEL} for both **AMPPD** and **CSPD**, the turnover number k_{cat} for the enzymatic dephosphorylation of the **AMPPD** was found to be (5.4 ± 0.9) × 10^3 s^{-1} and (4.6 ± 0.8) × 10^3 s^{-1} for **CSPD** at pH 9.0−10.5 and 37 °C.

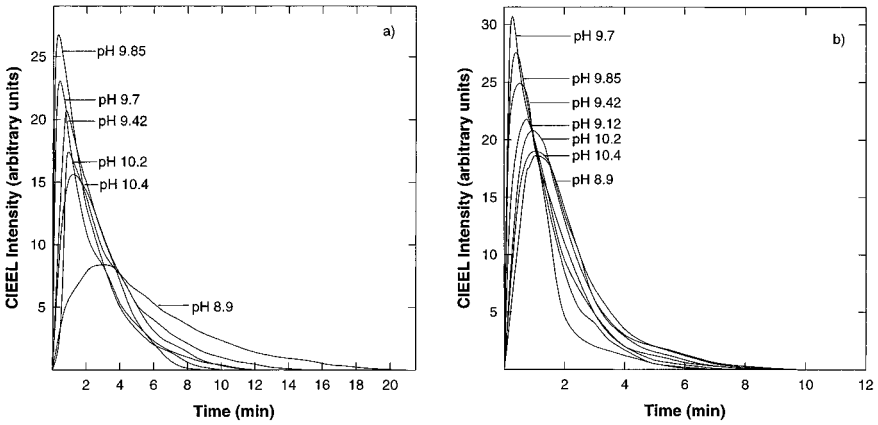

Figure 3. pH Dependence of the CIEEL kinetics in the decomposition of (a) **AMPPD** ([**AMPPD**] = 1.65×10^{-5} M) and (b) **CSPD** ([**CSPD**] = 1.85×10^{-5} M) catalyzed by alkaline phosphatase ([**AP**] = 10^{-8} M) in 0.05 M carbonate buffer, 1 mM $MgCl_2$ at 37 °C.

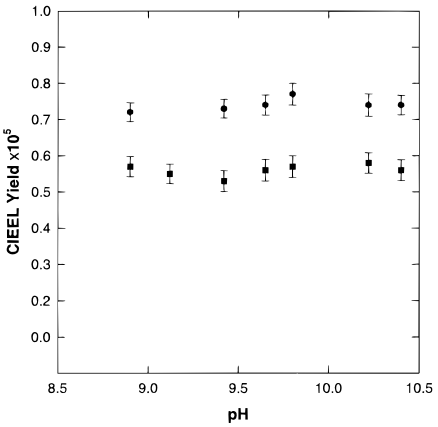

Figure 4. pH Dependence of the CIEEL yields in the alkaline-phosphatase-catalyzed decomposition of **AMPPD** (●) and **CSPD** (■) at the experimental conditions of Figure 3.

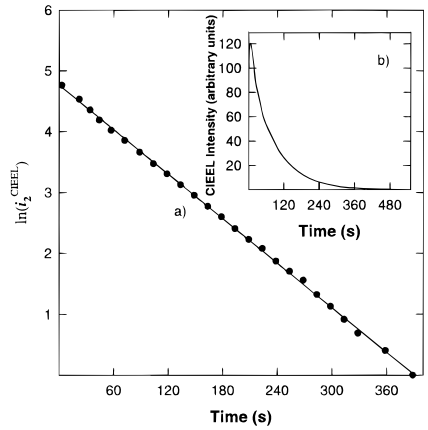

Figure 5. CIEEL decay of the **2a-H** ([**2a-H**]$_0$ = 2.42×10^{-5} M) decomposition induced by NaOH in water (pH 12.7) at 37 °C; first-order plot according to eq 8 (a) of the CIEEL intensity *versus* time data (b).

Discussion

All kinetic parameters for the enzymatic CIEEL process of Scheme 1, namely the CIEEL emitter fluorescence lifetime, the rate constant of the dioxetane anion **2** cleavage, the Michaelis constant, and the turnover number as well as the CIEEL efficiency were measured within the pH range at which alkaline phosphatase is catalytically active. At pH > 9, the Michaelis constant K_M depends on pH, whereas all the other parameters are independent of pH. To rationalize these experimental results, a detailed discussion of the interrelated processes in Scheme 1, namely (i) phenolate **4** fluorescence, (ii) dioxetane anion **2** cleavage, and (iii) enzymatic catalysis at alkaline pH is essential.

In general, according to Scheme 1, protonation of the excited phenolate **4*** may form both the ground (**4-H**) and the excited state phenol species (**4-H***). The latter adiabatic proton transfer[12] would result in the new CIEEL emitter **4-H*** (Scheme 1). However, time-resolved fluorescence measurements showed that the role of the protonation of **4*** is negligible at alkaline pH since no difference in the phenolate **4*** fluorescence lifetimes at various alkaline pH was observed (Figure 2). This lack of pH dependence of the phenolate **4** fluorescence lifetime τ can be justified through a conventional Stern−Volmer analysis at alkaline conditions.

Let us consider protonation of the excited phenolate **4*** as its quenching by H^+ with the overall quenching rate constant k_q, irrespective of whether such process results in the ground or excited state phenol species **4-H** and **4-H***. In the presence of H^+, the conventional Stern−Volmer expression for the fluorescence lifetime is given by $\tau = \tau_0/(1 + k_q\tau_0[H^+])$, where τ_0 represents the lifetime of **4*** at negligible $[H^+]$. Comparison of τ and τ_0 allows us to assess how significant the protonation of **4*** is at a given pH by estimating τ_0 from the experimental data available for τ. The upper limit of the quenching effect of the phenolate **4*** through its protonation would require the rate constant k_q of this process to be a diffusion-controlled (*ca.* 10^{10} M^{-1} s^{-1}), which means that at pH 9, for example, and the experimental value τ *ca.* 10 ns (Figure 2), $\tau = \tau_0/(1 + 10\tau_0) \approx 10^{-8}$ s. Therefore, $\tau_0 \approx 10^{-8}/(1-10^{-7}) \approx 10^{-8}$ s, *i.e.*, there is no difference in the lifetime values at pH 9 and in the absence of protons. This implies that in the applied pH range 9.0−10.5, protonation of the excited phenolate **4*** is negligible because of its short lifetime. Hence, under alkaline conditions, neither the nature of the CIEEL emitter phenolate **4*** nor its fluorescence lifetime and, therefore, its fluorescence efficiency are affected by pH.

The chemiexcitation step (**2** → **4*** in Scheme 1) consists of the elementary act of the cleavage of the dioxetane **2** and is expectedly independent of pH. Therefore, pH may affect the CIEEL yield only by changes of the fluorescence efficiency of the CIEEL emitter. However, we have just shown that pH does not affect the fluorescence efficiency and, therefore, pH should not affect the CIEEL yield as well as experimentally established in Figure 4.

Thus, under alkaline conditions, the fate of the CIEEL emitter is independent of pH because of its short lifetime (τ *ca.* 10 ns). On the contrary, its precursor, the dioxetane phenolate **2** is a long-lived species. Indeed, from the pseudo-first-order

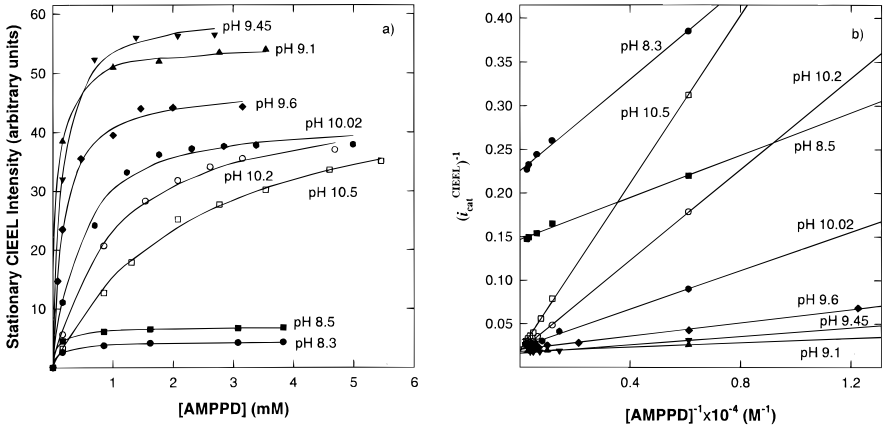

Figure 6. CIEEL in the decomposition of **AMPPD** catalyzed by alkaline phosphatase ([**AP**] = 4.7×10^{-13} M) in 0.05 M carbonate buffer, 1 mM $MgCl_2$ at 37 °C and at various pH: (a) intensity *versus* **AMPPD** concentration and (b) double-reciprocal plot according to eq 6.

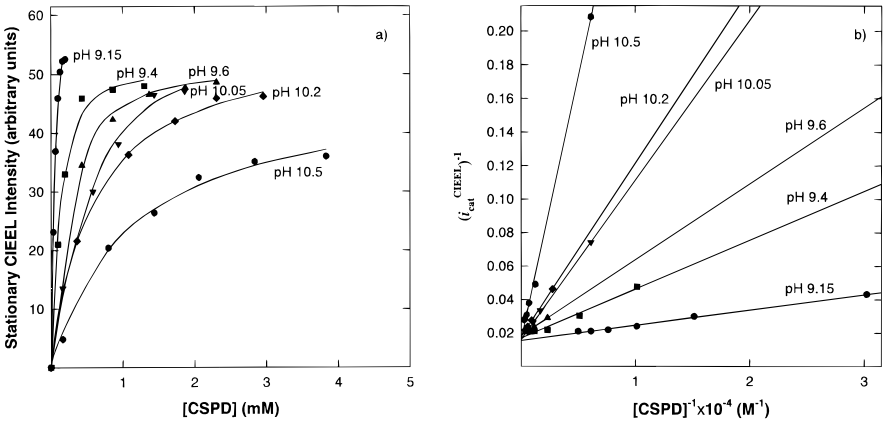

Figure 7. CIEEL in the decomposition of **CSPD** catalyzed by alkaline phosphatase ([**AP**] = 4.7×10^{-13} M) in 0.05 M carbonate buffer, 1 mM $MgCl_2$ at 37 °C and at various pH; (a) intensity *versus* **CSPD** concentration and (b) double-reciprocal plot according to eq 6.

CIEEL decay at high pH (Figure 5), the rate constant k_3 of the dioxetane **2a** cleavage is $(1.2 \pm 0.04) \times 10^{-2}$ s^{-1} at 37 °C., which corresponds to a half-life ($\tau_{1/2} = \ln 2/k_3$) of *ca.*1 min. This means that participation of **2** in bimolecular processes such as its rephosphorylation and protonation (Scheme 3) may be very probable. These possibilities need now to be scrutinized.

Unfortunately, involvement of the rephosphorylation step k_{-2} in Scheme 3 makes for very complex kinetics. However, knowledge of the rate constant k_3 should allow us to decide whether step k_{-2} in Scheme 3 can be neglected and thereby phosphorylation of the enzyme considered to be irreversible. Such a simplification makes the kinetic analysis of the enzymatic triggering process amenable. Let us compare the rates of the two competitive steps k_3 *versus* k_{-2}, which are the cleavage of the dioxetane **2** and its rephosphorylation. If, according to Scheme 2, the three forms $\mathbf{E}H_2^{2+}$, $\mathbf{E}H^+$, and **E** of the free enzyme are considered, of which only form $\mathbf{E}H^+$ is catalytically active, the rate of rephosphorylation is given by the expression $k_{-2}[\mathbf{2}][\mathbf{E}H^+{\cdot}PO_3^-]$, while the cleavage rate of **2** is $k_3[\mathbf{2}]$. Since [**2**] in both rate expressions is the same, one needs to compare the values for $k_{-2}[\mathbf{E}H^+{\cdot}PO_3^-]$ and k_3 (*ca.*10^{-2} s^{-1}). The upper limit for the value $k_{-2}[\mathbf{E}H^+{\cdot}PO_3^-]$ would require k_{-2} to be diffusion-controlled (*ca.*10^{10} M^{-1} s^{-1}) and $[\mathbf{E}H^+{\cdot}PO_3^-]$ to be equal to the initial, total enzyme concentration e_0 (*ca.* 10^{-13} M), which would amount to *ca.* 10^{-3} s^{-1}. Thus, even the upper limit of $k_{-2}[EH^+{\cdot}PO_3^-]$ is by about an order of magnitude smaller than k_3. The real $k_{-2}[\mathbf{E}H^+{\cdot}PO_3^-]$ value should be much less than 10^{-3} s^{-1}, since very probably k_{-2} is less than diffusion-controlled and $[\mathbf{E}H^+{\cdot}PO_3^-]$ should be much lower than the total enzyme concentration e_0. For the latter, not all of the enzyme molecules are catalytically active and, moreover, not all of catalytically active enzyme molecules are phosphorylated, *i.e.*, $[\mathbf{E}H^+{\cdot}PO_3^-] < [\mathbf{E}H^+] < e_0$ (*ca.* 10^{-13} M). Consequently, for the intermediate **2a**, it follows that $k_{-2}[\mathbf{E}H^+{\cdot}PO_3^-] \ll k_3$, while for the chloro-substituted dioxetane intermediate **2b**, this inequality is even more pronounced. Indeed, it was previously found[9] that chloro substitution leads to faster cleavage of **2** in every medium studied. Therefore, one can neglect the rate of the rephosphorylation (k_{-2}) in comparison with the rate of the dioxetane **2** cleavage (k_3) and thereby consider phosphorylation of the enzyme ($\boldsymbol{k}_2$) in the Michaelis complex (Scheme 3) as an irreversible step, which considerably simplifies the kinetics of the enzymatic triggering process.

Scheme 4

$$\mathbf{2} + H_2O \underset{k_{-5}}{\overset{k_5}{\rightleftharpoons}} \mathbf{2\text{-}H} + HO^-$$

$$\mathbf{2\text{-}H} + H_2O \underset{k'_5}{\overset{k'_{-5}}{\rightleftharpoons}} \mathbf{2} + H_3O^+$$

The influence of protonation of the intermediate **2** on its stationary concentration and thereby CIEEL intensity may be understood through the following kinetic analysis. According to Scheme 4, the pseudo-constants $\tilde{k}_5$ of the protonation of the dioxetane phenolate **2** and $\tilde{k}_5$ of the deprotonation of the phenol **2-H** in aqueous buffer may be defined by eqs 9 and 10. Neglect of the rephosphorylation step k_{-2} in Scheme 3 gives eqs 11 and 12 for the concentrations of **2** and **2-H** under the steady-state conditions. Solution of eqs 11 and 12 in terms of [**2**] results in eq 13, from which one can see that under these circum-

$$\tilde{k}_5 = k_5[H_2O] + k'_5[H^+] \quad (9)$$

$$\tilde{k}_{-5} = k_{-5}[HO^-] + k'_{-5}[H_2O] \quad (10)$$

$$\frac{d[\mathbf{2}]}{dt} = v_{cat} + \tilde{k}_{-5}[\mathbf{2\text{-}H}] - (\tilde{k}_5 + k_3)[\mathbf{2}] = 0 \quad (11)$$

$$\frac{d[\mathbf{2\text{-}H}]}{dt} = \tilde{k}_5[\mathbf{2}] - \tilde{k}_{-5}[\mathbf{2\text{-}H}] = 0 \quad (12)$$

$$v_{cat} = k_3[\mathbf{2}] \quad (13)$$

stances, the concentration of the dioxetane phenolate **2** is equal to v_{cat}/k_3. Thus, under the steady-state conditions, the protonation of **2** and the deprotonation of **2-H** do not affect the dioxetane **2** concentration and thereby the stationary CIEEL intensity.

To understand how enzymatic dephosphorylation of the dioxetanes **AMPPD** and **CSPD** depends on pH, the experimental data on the catalytic parameters k_{cat} and K_M *versus* pH need to be examined in terms of Scheme 3. The k_{cat} value of *ca.* 5×10^3 s^{-1} shows rapid turnover of the alkaline phosphatase for both **AMPPD** and **CSPD**. As to the question whether k_{cat} is pH dependent, we had shown that the value $\Phi^{CIEEL}e_0k_{cat}$ is independent of pH within the entire pH range (9.0−10.5) at which the alkaline phosphatase catalyzes effectively. Indeed, the intercept $(\Phi^{CIEEL}e_0k_{cat})^{-1}$ of the double-reciprocal plot according to eq 6 (Figures 6b and 7b) was found to be independent of pH within the pH range of 9.0−10.5. Since Φ^{CIEEL} is also independent of pH, it follows that k_{cat} is independent as well. Thus, for the entire pH range employed here, k_{cat} is *ca.* 5×10^3 s^{-1}. Only at pH lower than 9, the intercept $(\Phi^{CIEEL}e_0k_{cat})^{-1}$ of the double-reciprocal plot (Figure 6b) increases markedly with decreasing pH, which reflects the decrease of the k_{cat} since Φ^{CIEEL} and e_0 are constant values. Similar pH dependence of the k_{cat} is known for the hydrolysis of *p*-nitrophenylphosphate by intestinal alkaline phosphatase.[17]

In contrast to the turnover number (k_{cat}), the Michaelis constant (K_M) depends on pH within the entire pH range used. To understand this pH behavior of the catalytic parameters k_{cat} and K_M, one must take into account the existence of various forms of the free enzyme. According to Scheme 2, the concentrations of the three forms $\mathbf{E}H_2^{2+}$, $\mathbf{E}H^+$, and **E** of the free enzyme can be related with one another by the ionization constants[15,21] K_{a_1} and K_{a_2} defined by eqs 14 and 15. This leads to eq 16 for the total enzyme concentration e_0 as a sum of the concentrations of all free enzyme forms, from which it follows that the concentration of the catalytically active enzyme form $\mathbf{E}H^+$ in the absence of substrate is given by eq 17.

$$K_{a_1} = \frac{[\mathbf{E}H^+][H^+]}{[\mathbf{E}H_2^{2+}]} \quad (14)$$

$$K_{a_2} = \frac{[\mathbf{E}][H^+]}{[\mathbf{E}H^+]} \quad (15)$$

$$e_0 = [\mathbf{E}H_2^{2+}] + [\mathbf{E}H^+] + [\mathbf{E}] = [\mathbf{E}H^+]\left\{1 + \frac{[H^+]}{K_{a_1}} + \frac{K_{a_2}}{[H^+]}\right\} \quad (16)$$

$$[\mathbf{E}H^+] = \frac{e_0}{1 + \frac{[H^+]}{K_{a_1}} + \frac{K_{a_2}}{[H^+]}} \quad (17)$$

(21) Mathews, C. K.; van Holde, K. E. *Biochemistry*; The Benjamin/Cummings Publishing Co: Redword City, 1990; pp 43−137.

In the presence of the dioxetane **1** as substrate, the Michaelis complex $\mathbf{E}H^+\cdot\mathbf{1}$ and the phosphorylated enzyme $\mathbf{E}H^+\cdot PO_3^-$ need to be considered in addition to the free enzyme forms. According to Scheme 3, and neglect of the dioxetane rephosphorylation step k_{-2}, the concentrations of $\mathbf{E}H^+\cdot\mathbf{1}$ and $\mathbf{E}H^+\cdot PO_3^-$ under the steady-state conditions are expressed by eqs 18 and 19. From eq 18 one obtains eq 20, which relates $[\mathbf{E}H^+]$ with $[\mathbf{E}H^+\cdot\mathbf{1}]$, and eq 19 gives similarly eq 21 for $[\mathbf{E}H^+\cdot PO_3^-]$ and $[\mathbf{E}H^+\cdot\mathbf{1}]$.

$$\frac{d[\mathbf{E}H^+\cdot\mathbf{1}]}{dt} = k_1[\mathbf{E}H^+][\mathbf{1}] - (k_{-1} + k_2)[\mathbf{E}H^+\cdot\mathbf{1}] = 0 \quad (18)$$

$$\frac{d[\mathbf{E}H^+\cdot PO_3^-]}{dt} = k_2[\mathbf{E}H^+\cdot\mathbf{1}] - k_4[HO^-][\mathbf{E}H^+\cdot PO_3^-] = 0 \quad (19)$$

$$[\mathbf{E}H^+] = \frac{(k_{-1} + k_2)[\mathbf{E}H^+\cdot\mathbf{1}]}{k_1[\mathbf{1}]} \quad (20)$$

$$[\mathbf{E}H^+\cdot PO_3^-] = \frac{k_2}{k_4[HO^-]}[\mathbf{E}H^+\cdot\mathbf{1}] \quad (21)$$

$$e_0 = [\mathbf{E}H^+]\left\{1 + \frac{[H^+]}{K_{a_1}} + \frac{K_{a_2}}{[H^+]}\right\} + [\mathbf{E}H^+\cdot\mathbf{1}] + [\mathbf{E}H^+\cdot PO_3^-] \quad (22)$$

In the presence of the substrate **1**, the total enzyme concentration e_0 consists of the sum of the concentrations of all its forms, namely $\mathbf{E}H_2^{2+}$, $\mathbf{E}H^+$, **E**, $\mathbf{E}H^+\cdot\mathbf{1}$, and $\mathbf{E}H^+\cdot PO_3^-$, which is expressed in eq 22. Solution of eqs 20−22 results in eq 23 for the concentration of the Michaelis complex. The rate of the catalytic generation of the CIEEL-active dioxetane **2** through enzymatic dephosphorylation (Schemes 3) can be obtained from eq 23 by multiplication of the latter by the rate constant $\boldsymbol{k}_2$, which leads to eq 24. Comparison of eq 24 with the Michaelis-Menten eq 4 leads to expressions for the catalytic parameters k_{cat} and K_M in the form of eqs 25 and 26, which account for the experimentally observed pH influence.

$$[\mathbf{E}H^+\cdot\mathbf{1}] = \frac{e_0[\mathbf{1}]}{\left(1 + \frac{k_2}{k_4[HO^-]}\right)\left\{[\mathbf{1}] + \frac{k_{-1} + k_2}{k_1\left(1 + \frac{k_2}{k_4[HO^-]}\right)}\left(1 + \frac{[H^+]}{K_{a_1}} + \frac{K_{a_1}}{[H^+]}\right)\right\}} \quad (23)$$

$$v_{cat} = \frac{k_2e_0[\mathbf{1}]}{\left(1 + \frac{k_2}{k_4[HO^-]}\right)\left\{[\mathbf{1}] + \frac{k_{-1} + k_2}{k_1\left(1 + \frac{k_2}{k_4[HO^-]}\right)}\left(1 + \frac{[H^+]}{K_{a_1}} + \frac{K_{a_2}}{[H^+]}\right)\right\}} \quad (24)$$

$$k_{cat} = \frac{k_2}{1 + \frac{k_2}{k_4[HO^-]}} \quad (25)$$

$$K_M = \frac{k_{-1} + k_2}{k_1\left(1 + \frac{k_2}{k_4[HO^-]}\right)}\left\{1 + \frac{[H^+]}{K_{a_1}} + \frac{K_{a_2}}{[H^+]}\right\} \quad (26)$$

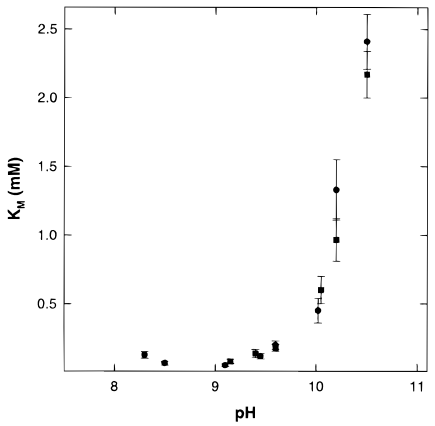

Figure 8. pH Dependence of the Michaelis constant for the alkaline-phosphatase-catalyzed decomposition of **AMPPD** (●) and **CSPD** (■) in 0.05 M carbonate buffer at 37 °C, 1 mM $MgCl_2$ and 4.7×10^{-13} M alkaline phosphatase.

Indeed, the lack of pH dependence of the k_{cat} at pH > 9 suggests that at high pH the rate-limiting step is the phosphorylation of the enzyme, whereas the regeneration of the free catalytically active enzyme form $\mathbf{E}H^+$ through the pH-controlled dephosphorylation of $\mathbf{E}H^+ \cdot PO_3^-$ is fast, since $k_4[HO^-]$ is high enough. This reduces eq 25 to its limiting case shown in eq 27, which is valid at pH > 9, *i.e.*, high $[HO^-]$. Similarly, at pH > 9, eq 26 for the Michaelis constant can be reduced to eq 28 as limiting case, since again $\boldsymbol{k}_4[HO^-]$ is sufficiently high.

$$k_{cat} \approx k_2 \tag{27}$$

$$K_M \approx \frac{k_{-1} + k_2}{k_1}\left\{1 + \frac{[H^+]}{K_{a_1}} + \frac{K_{a_2}}{[H^+]}\right\} \tag{28}$$

The pH dependence of the Michaelis constant K_M is thereby determined by the relative importance of the terms

$$\frac{[H^+]}{K_{a_1}}$$

and

$$\frac{K_{a_2}}{[H^+]}$$

in eq 28. The shape of the experimental pH dependence of the K_M (Figure 8) suggests that within the pH range used, the

$$\frac{K_{a_2}}{[H^+]}$$

term contributes mainly to K_M in eq 28 since it is this term which is responsible for the increase of the K_M (Figure 8) with increasing pH (decreasing $[H^+]$). In terms of Scheme 2, the latter fact is presumably associated with the decrease of the concentration of the active enzyme form $\mathbf{E}H^+$ through its deprotonation at increasing pH.

From the above detailed kinetic analysis of the experimental data on the enzymatic triggering of dioxetanes **1** we observe that although every step of the triggering process in Schemes 1 and 3 involves either H^+ or HO^- ions, at alkaline pH and steady-state conditions, only the enzymatic dephosphorylation of the **AMPPD** and **CSPD** depends on pH in this CIEEL process. The turnover number (k_{cat}) is affected only at pH below 9, which reflects a switchover of the rate-determining step of the enzyme dephosphorylation to its phosphorylation (Scheme 3) at increasing pH and is described by eq 25 and its limiting form of eq 27. The Michaelis constant (K_M) depends on pH within the entire pH range used, which may be attributed to the pH effect on the concentration of the catalytically active enzyme form.

We conclude that the protonation of **2** and the deprotonation of **2-H** do not affect the CIEEL intensity under steady-state conditions and the CIEEL efficiency is independent of pH. Fortunately, the neglect of the dioxetane rephosphorylation step k_{-2} (Scheme 3) at alkaline pH simplifies the kinetics of the CIEEL process sufficiently to permit a complete analysis. Such kinetic analysis provides the essential mechanistic insight for the design of novel enzyme-triggered CIEEL-active probes. Particularly when target molecules (proteins or nucleic acids) are attached to the enzyme, the catalytic properties of the latter are expected to be affected through the pH dependence of both the turnover number (k_{cat}) and the Michaelis constant (K_M) compared with those of the free enzyme. Therefore, the pH conditions should be optimized for every particular enzyme-triggered chemiluminescent probe through a detailed kinetic analysis, especially when enzymes immobilized on membranes and water-soluble polymers are employed.

Acknowledgment. Generous funding by the Deutsche Forschungsgemeinschaft (Sonderforschungsbereich 172 "Molekulare Mechanismen kanzerogener Primärveränderungen") is gratefully appreciated. A.V.T. and R.F.V. thank also the Rossiiskii Fond Fundamental'nykh Issledovanii (Grant No. 96-03-34142) and the International Science Foundation (Grant JIL 100) for the financial support. We thank Dr. C. R. Saha-Möller, Dr. J. C. Voyta, and K. Mielke for many helpful discussions and comments.

Supporting Information Available: Experimental procedures (2 pages). See any current masthead page for ordering and Internet access instructions.

JA961904G